

## ZnO nanorods for solar cells: Hydrothermal growth versus vapor deposition

Y. F. Hsu,<sup>1</sup> Y. Y. Xi,<sup>1</sup> A. B. Djurišić,<sup>1,a)</sup> and W. K. Chan<sup>2</sup>

<sup>1</sup>Department of Physics, The University of Hong Kong, Pokfulam Road, Hong Kong

<sup>2</sup>Department of Chemistry, The University of Hong Kong, Pokfulam Road, Hong Kong

(Received 26 January 2008; accepted 17 March 2008; published online 2 April 2008)

Performance of dye-sensitized solar cells (DSSCs) based on ZnO nanorods prepared by hydrothermal and vapor-deposition methods has been investigated. In spite of their inferior optical properties, DSSCs based on hydrothermally grown rods exhibit higher power conversion efficiency, which can be attributed to the higher dye adsorption. Hydrothermally grown and vapor deposited nanorods also exhibit different dependence of photovoltaic performance on the annealing conditions of the rods, indicating significant effect of the native defects on the achievable photocurrent and power conversion efficiency. Efficiency of 0.22% is obtained for both as grown hydrothermally grown nanorods and vapor deposited nanorods annealed in oxygen at 200 °C. © 2008 American Institute of Physics. [DOI: 10.1063/1.2906370]

Dye-sensitized solar cells (DSSCs) based on TiO<sub>2</sub> nanoparticle network<sup>1</sup> usually consist of an oxide layer which serves as the photoanode, a dye which serves as the light absorber and an organic solvent containing redox system. While nanoparticle network films have a large surface area, the electron transport in these cells is trap mediated and consequently very slow.<sup>2</sup> To address this issue, DSSCs based on one-dimensional nanostructures, such as ZnO nanowires,<sup>2</sup> have been recently attracting increasing attention. While ZnO nanowires exhibit significantly higher electron mobility compared to both TiO<sub>2</sub> and ZnO nanoparticle films, power conversion efficiency of a DSSC based on 20 μm long ZnO nanowires was only 1.5%.<sup>2</sup> Various approaches have been used to improve the cell efficiency, such as using ZnO–TiO<sub>2</sub> core-shell nanowires<sup>3</sup> and increasing the surface area of the ZnO by using branched structures<sup>4,5</sup> or mixed nanowire/nanoparticle morphologies.<sup>6</sup>

While it is clear that increasing the surface area of the cell while maintaining the efficient electrical transport in nanowires improves the cell efficiency,<sup>4–6</sup> there are many possible methods to fabricate ZnO nanomaterials, but their properties are strongly dependent on the fabrication conditions used. The range of the reported efficiencies for ZnO-based DSSCs fabricated using different methods<sup>2,4–7</sup> is very wide, but these efficiencies cannot be directly compared due to the differences in active layer thickness and the morphology of the active layer. For example, for hydrothermally grown nanorods (using different conditions), reported efficiencies were 0.84% for 5.5 μm,<sup>6</sup> 1.0% for 11 μm,<sup>4</sup> and 1.5% for 20 μm<sup>2</sup> long rods. On the other hand, for vapor deposited rods (5–6 μm length) the obtained power conversion efficiency was 0.34%.<sup>5</sup> It has also been shown that photovoltaic response of ZnO nanorods is dependent not only on the rod size but also on their orientation.<sup>8</sup> While hydrothermal growth has the advantage of being simple and inexpensive,<sup>9</sup> concentration of defects in hydrothermally grown ZnO nanorods is usually large<sup>10</sup> and they typically exhibit inferior material quality compared to vapor deposited samples.<sup>11</sup> Thus, it is of interest to compare the photovoltaic performance of the rods grown by the two methods, and also

investigate effects of annealing since postfabrication annealing has been shown to affect optical<sup>10,12</sup> and electronic<sup>13</sup> properties of ZnO nanorods.

ZnO nanorods were grown on fluorine doped tin oxide (FTO)/quartz substrates (Solaronix). For hydrothermal growth, seed layer was prepared using zinc acetate solution and annealed at 350 °C.<sup>9,10</sup> The substrates covered with the seed layer were then placed upside down in a 75 mL aqueous growth solution containing 0.1 g polyethylene (Aldrich, 50 wt % in water), 25 mM zinc nitrate hydrate (Aldrich, 99.999%), and hexamethylenetetramine (Aldrich, 99+%).<sup>10</sup> The reaction time was 10 h, with the replacement of fresh solution every 2.5 h.<sup>9</sup> For rods fabricated by vapor deposition, the substrates were placed 1.5 cm above Zn source (0.2 g, Aldrich, ~100 mesh, 99.998%). The reaction was performed in a horizontal tube furnace with a base pressure (no gas flow) in the order of 10<sup>-2</sup> Torr. Before the start of the growth, the furnace was flushed with 0.1 L/m argon gas. When the furnace reached 500 °C, a flow of 0.01 L/m oxygen gas was added. The pressure during growth was 1 Torr, and the reaction time was 1.5 h. Annealing was performed in a tube furnace under the flow of 0.1 L/m oxygen or forming gas at different temperatures (200, 400, and 600 °C).

The morphology of the rods was studied by using Leo 1530 field emission scanning electron microscopy (SEM), while the optical properties were studied by photoluminescence (PL) spectroscopy using HeCd laser (325 nm) as the excitation source. The flat band potential (corresponding to aqueous solution with pH=6) and carrier concentration were determined by electrochemical impedance spectroscopy measurement using an Autolab electrochemistry working station (PGSTAT-30). The measurements were performed in a sodium sulphate (Na<sub>2</sub>SO<sub>4</sub>, Uni-Chem, Anhydrous) aqueous solution with a three electrode configuration using a Pt wire as the counter electrode and the Ag/AgCl (in 3M KCl) as the reference electrode, and the measurement was done applying a 10 mV amplitude ac signal over the constant applied bias with the frequency ranging between 100 kHz and 50 mHz.

For DSSC fabrication, the samples were immersed into a 5 mM ethanolic solution of the dye *cis*-bis(isothiocyanato)bis(2,2'-bipyridyl-4,4'-dicarboxy lato)-ruthenium(II) bis-tetrabutylammonium (N719) (Solaronix)

<sup>a)</sup>Electronic mail: dalek@hkusua.hku.hk.

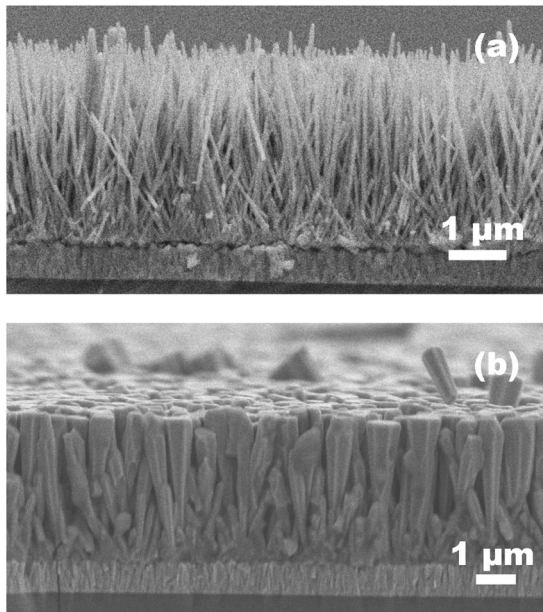


FIG. 1. SEM images of ZnO nanorods grown by (a) hydrothermal method and (b) vapor deposition.

which was kept at 80 °C for 2 h. The solar cells were assembled using an electrolyte containing 0.5M LiI (Fluka), 0.05M I<sub>2</sub> (Fluka) (redox system), and 0.5M 4-tertbutylpyridine (Fluka) (an ionic electrolyte which can improve the charge transport and increase the  $V_{oc}$ )<sup>14</sup> in 3-methoxypropionitrile solvent (Fluka), and a platinum coated conductive oxide glass (Solaronix) as a counter electrode. The performance of a DSSC is affected by the properties of metal oxide, as well as the choice of dye and electrolyte. To investigate the influence of oxide properties on the cell performance, dye and electrolyte were kept the same in all devices and were chosen based on previous reports on efficient ZnO nanorod based cells.<sup>2</sup> The  $I$ - $V$  curves were measured by Keithley 2400 sourcemeter under the illumination of an Oriol 66002 solar light simulator (at 100 mW cm<sup>-2</sup>), using 1.5 AM light. The active electrode area was 0.385 cm<sup>2</sup>. Before performing desorption measurements, the samples after dye loading were rinsed in ethanol to remove residual dye on the rods and then immersed into 0.1 mM KOH solution ( $pH \sim 9$ ) for at least 30 min to desorb and fully deprotonate the dye. The absorbance of the resulting solutions was measured using a Cary 50 Bio UV-vis spectrophotometer.

Figure 1 shows the morphology of the rods grown by hydrothermal and vapor deposition methods. While the morphologies on Si substrates are similar (not shown), on FTO substrates vapor deposited rods exhibit increasing diameter with increasing length. Thus, for both growth methods we have limited the rod length to  $\sim 3.5 \mu\text{m}$  due to close packing of the top area of the vapor deposited rods, although increased rod length would result in higher efficiencies for hydrothermally grown rods. Due to differences in the rod morphology, we have measured both photovoltaic performance and determined differences in the dye loading.

Figure 2 shows the  $I$ - $V$  curves of DSSCs based on hydrothermally grown ZnO nanorods annealed in different environments. For both oxygen (oxidizing environment) and forming gas (reducing environment), similar trends are observed. Thus, we will mainly focus on oxygen annealing,

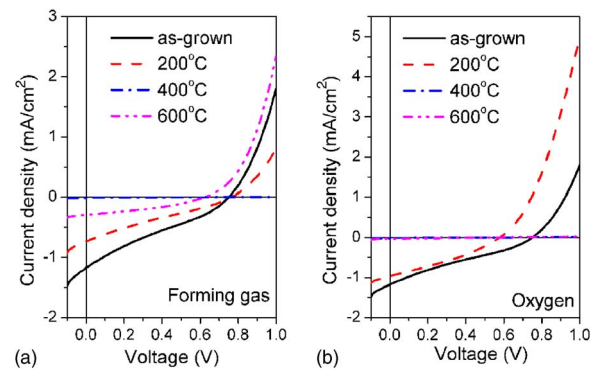


FIG. 2. (Color online)  $I$ - $V$  curves under 1.5AM simulated solar illumination of ZnO nanorods grown by hydrothermal method (a) annealed in oxygen and (b) annealed in forming gas.

since it does not result in the damage of the rod morphology unlike annealing in forming gas flow.<sup>12</sup> Hydrothermally grown nanorods without any further treatment exhibit the power conversion efficiency of  $\eta=0.22\%$ , with open circuit voltage  $V_{oc}=0.76$  V, short circuit current density  $I_{sc}=1.17$  mA/cm<sup>2</sup>, and fill factor  $FF=0.25$ . The annealing results in a significant decrease of open circuit voltage and short circuit current density, while the fill factor shows small increase for annealing at 200 and 600 °C. Overall, the achieved efficiencies are  $\eta=0.18\%$  for 200 °C, 0.001% for 400 °C, and 0.07% for 600 °C. The open circuit voltage exhibits significant decrease from 0.76 V in as grown cells to  $V_{oc}=0.58$  V for 200 °C,  $V_{oc}=0.52$  V for 400 °C, and  $V_{oc}=0.53$  V for 600 °C. Worsening of the cell performance for annealing at higher temperatures (400 and 600 °C) is also observed for DSSC cells with vapor deposited ZnO nanorods, as shown in Fig. 3(a). We can also observe similar drop in the open circuit voltage, from  $V_{oc}=0.66$  V for as grown nanorods, to  $V_{oc}=0.60$  V for 200 °C,  $V_{oc}=0.51$  V for 400 °C, and  $V_{oc}=0.45$  V for 600 °C. Different from hydrothermally grown nanorods, cell performance is the worst for annealing at 600 °C ( $\eta=0.02\%$ ), followed by annealing at 400 °C ( $\eta=0.08\%$ ). As grown nanorods exhibited  $I_{sc}=0.37$  mA/cm<sup>2</sup>, and  $FF=0.39$ , resulting in overall efficiency of 0.09%. After annealing in oxygen at 200 °C,  $I_{sc}$  increased to 1.01 mA/cm<sup>2</sup>, while  $FF=0.37$ , resulting in overall efficiency of 0.22%.

PL spectra of the nanorods grown by hydrothermal method and vapor deposition after annealing at different conditions are shown in Figs. 3(b) and 3(c), respectively. We can observe that the samples with the lowest UV-vis emission ratio exhibit the highest efficiency. However, there is no simple correlation between the UV-vis emission ratio and photovoltaic performance, since hydrothermally grown nanorods annealed at 400 °C exhibited higher visible emission and lower power conversion efficiency compared to samples annealed at 200 and 600 °C.

To investigate the reasons for the decrease of the  $V_{oc}$  with annealing, electrochemical impedance measurements were performed and the positions of the flat band potential and carrier concentrations were calculated.<sup>15</sup> However, for the hydrothermally grown rods the data could not be fitted with a straight line, which was likely related to the small size of the rods since the rod dimension should be greater than the depletion region width.<sup>15</sup> In addition, the high density of the surface states may also affect the obtained results.<sup>15</sup> For vapor deposited rods, however, linear dependence in agree-

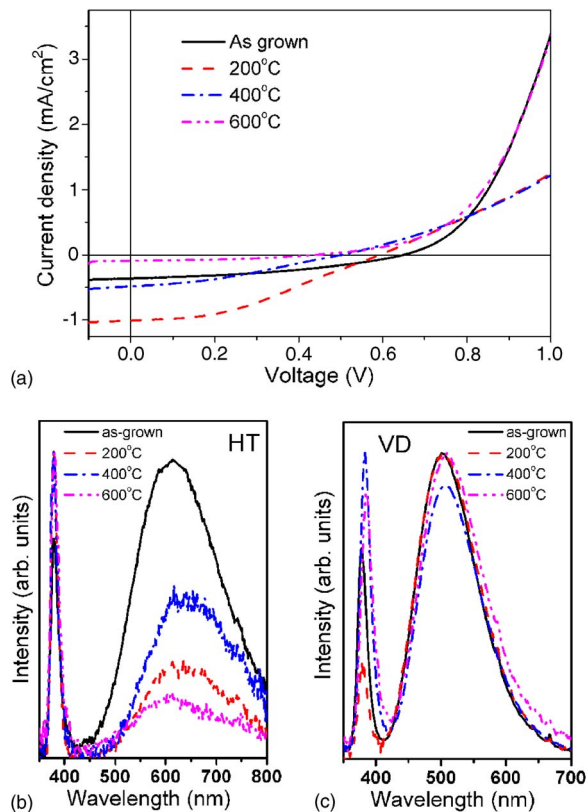


FIG. 3. (Color online)  $I$ - $V$  curves under 1.5AM simulated solar illumination of ZnO nanorods grown by vapor deposition and annealed in oxygen. (b) PL of ZnO nanorods grown by hydrothermal method for different annealing conditions. (c) PL of ZnO nanorods grown by vapor deposition for different annealing conditions.

ment with the Mott-Schottky equation is obtained, and the calculated results for the flat band potential and carrier concentration are  $(-4.28 \pm 0.012)$  eV and  $(5.20 \pm 0.05) \times 10^{17} \text{ cm}^{-3}$  (as grown),  $-4.42 \pm 0.012$  eV and  $(3.37 \pm 0.04) \times 10^{17} \text{ cm}^{-3}$  (200 °C),  $(-4.56 \pm 0.007)$  eV and  $(1.00 \pm 0.01) \times 10^{17} \text{ cm}^{-3}$  (400 °C), and  $(-4.60 \pm 0.006)$  eV and  $(3.20 \pm 0.05) \times 10^{16} \text{ cm}^{-3}$  (600 °C). We can observe that the shift in the flat band potential follows the trends observed for the change in the  $V_{oc}$ . The large change observed for as grown rods and annealing at 200 °C may be related to the presence of the OH groups on the surface of the ZnO, which desorb after annealing at temperatures of 150 °C and above.<sup>10</sup>

Presence of the OH groups can also affect the dye loading, based on the obtained results for TiO<sub>2</sub> nanoparticles.<sup>16</sup> Due to this and the observed difference in the nanorod sizes, dye loading was investigated and the obtained results for the absorbance of the desorbed dye are shown in Fig. 4. The highest dye loading is obtained for hydrothermally grown rods without annealing, followed by vapor deposited rods annealed at 200 °C, which illustrates the fact that the dye loading also depends on the surface conditions and not only on the available surface area. In addition, for samples with small differences in dye loading, higher efficiency can be obtained for a sample with slightly smaller dye loading. This is likely due to the differences in charge collection efficiencies. Unlike nanoparticle networks, nanowires exhibit internal electric field which assists in the electron collection.<sup>2</sup> The depletion region width and the internal electric field would be dependent on the native defect concentrations (and con-

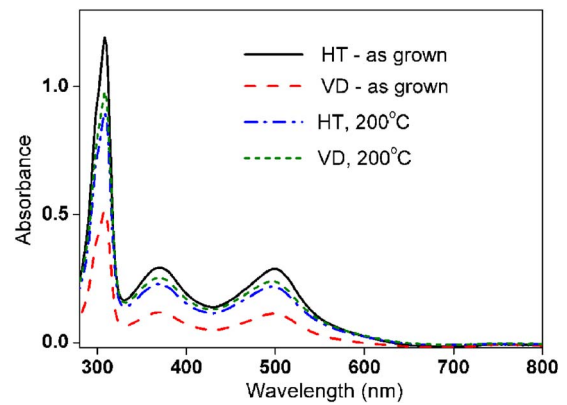


FIG. 4. (Color online) Absorbance of the dye desorbed from ZnO nanorods for different fabrication methods and annealing conditions.

sequently carrier concentrations) in the nanorods, so that the relationship between the rod properties and photovoltaic performance is complex.

To summarize, we investigated the photovoltaic performance of the DSSCs based on ZnO nanorods grown by two different methods. We found that the growth method and the resulting optical and electronic properties of the nanorods play a significant role in the photovoltaic performance. The photovoltaic performance exhibits a complex relationship to the presence of surface OH groups and defect emissions, and optimal annealing conditions are strongly dependent on the growth method used.

This work was supported by the Research Grants Council of The Hong Kong Special Administrative Region, China (Project Nos. HKU 7021/03P, HKU 7019/04P, and HKU 7010/05P). Financial support from the Strategic Research Theme, University Development Fund, Seed Funding Grant, and Outstanding Young Researcher Award (administered by The University of Hong Kong) are also acknowledged.

- <sup>1</sup>B. O'Regan and M. Grätzel, *Nature (London)* **353**, 737 (1991).
- <sup>2</sup>M. Law, L. E. Greene, J. C. Johnson, R. Saykally, and P. Yang, *Nat. Mater.* **4**, 455 (2005).
- <sup>3</sup>M. Law, L. E. Greene, A. Radenović, T. Kuykendall, J. Liphardt, and P. Yang, *J. Phys. Chem. B* **110**, 22652 (2006).
- <sup>4</sup>C. Y. Jiang, X. W. Sun, G. Q. Lo, D. L. Kwong, and J. X. Wang, *Appl. Phys. Lett.* **90**, 263501 (2007).
- <sup>5</sup>D.-I. Suh, S.-Y. Lee, T.-H. Kim, J.-M. Chun, E. K. Suh, O.-B. Yang, and S.-K. Lee, *Chem. Phys. Lett.* **442**, 348 (2007).
- <sup>6</sup>C.-H. Ku and J.-J. Wu, *Appl. Phys. Lett.* **91**, 093117 (2007).
- <sup>7</sup>I.-D. Kim, J.-M. Hong, B. H. Lee, D. Y. Kim, E.-K. Jeon, D.-K. Choi, and D.-J. Yang, *Appl. Phys. Lett.* **91**, 163109 (2007).
- <sup>8</sup>Q. Zhao, T. Xie, L. Peng, Y. Lin, P. Wang, L. Peng, and D. Wang, *J. Phys. Chem. C* **111**, 17136 (2007).
- <sup>9</sup>L. E. Greene, M. Law, D. H. Tan, M. Montano, J. Goldberger, G. Somorjai, and P. Yang, *Nano Lett.* **5**, 1231 (2005).
- <sup>10</sup>K. H. Tam, C. K. Cheung, Y. H. Leung, A. B. Djurišić, C. C. Ling, C. D. Beling, S. Fung, W. M. Kwok, W. K. Chan, D. L. Phillips, L. Ding, and W. K. Ge, *J. Phys. Chem. B* **110**, 20865 (2006).
- <sup>11</sup>A. B. Djurišić and Y. H. Leung, *Small* **2**, 944 (2006).
- <sup>12</sup>W. M. Kwok, A. B. Djurišić, Y. H. Leung, D. Li, K. H. Tam, D. L. Phillips, and W. K. Chan, *Appl. Phys. Lett.* **89**, 183112 (2006).
- <sup>13</sup>Q. Zhao, X. Y. Xu, X. F. Song, X. Z. Zhang, D. P. Yu, C. P. Li, and L. Guo, *Appl. Phys. Lett.* **88**, 033102 (2006).
- <sup>14</sup>R. S. Mane, W. J. Lee, H. M. Pathan, and S.-H. Han, *J. Phys. Chem. B* **109**, 24254 (2005).
- <sup>15</sup>M. Parthasarathy, N. S. Ramgir, B. R. Sathe, I. S. Mulla, and V. K. Pillai, *J. Phys. Chem. C* **111**, 13092 (2007).
- <sup>16</sup>J. Takahashi, H. Itoh, S. Motai, and S. Shimada, *J. Mater. Sci.* **38**, 1695 (2007).